Title

Unravelling biogeochemical drivers of methylmercury production in an Arctic fen soil and a bog soil

Authors

Zhang, Lijie

Philben, Michael

Taş, Neslihan

et al.

Publication Date

2022-04-01

DOI

10.1016/j.envpol.2022.118878

Peer reviewed

Unravelling Biogeochemical Drivers of Methylmercury Production in an Arctic Fen Soil and a Bog Soil

Lijie Zhang[1#], Michael Philben[1], Neslihan Taş[2], Alexander Johs[1], Ziming Yang[3], Stan D. Wullschleger[1], David E Graham[4], Eric M Pierce[1], Baohua Gu[1]*

[1] Environmental Sciences Division, Oak Ridge National Laboratory, Oak Ridge, TN 37831, USA

[2] Climate and Ecosystem Sciences Division, Lawrence Berkeley National Laboratory

[3] Department of Chemistry, Oakland University, Rochester, MI, 48309, USA

[4] Biosciences Division, Oak Ridge National Laboratory, Oak Ridge, TN 37831, USA

Present address: Department of Chemistry and Environmental Science, New Jersey Institute of Technology, Newark, NJ 07102, USA

* Corresponding author: Baohua Gu, Telephone: (865)-574-7286; E-mail: gub1@ornl.gov.

Abstract

Arctic tundra soils store a globally significant amount of mercury (Hg), which could be transformed to the neurotoxic methylmercury (MeHg) upon warming and thus poses serious threats to the Arctic ecosystem. However, our knowledge of the biogeochemical drivers of MeHg production is limited in these soils. Using substrate addition (acetate and sulfate) and selective microbial inhibition approaches, we investigated the geochemical drivers and dominant microbial methylators in 60-day microcosm incubations with two Arctic tundra soils: a circumneutral fen soil and an acidic bog soil, collected near Nome, Alaska, United States. Results showed that increasing acetate concentration had negligible influences on MeHg production in both soils. However, inhibition of sulfate-reducing bacteria (SRB) completely stalled MeHg production in the fen soil in the first 15 days, whereas addition of sulfate in the low-sulfate bog soil increased MeHg production by 5-fold, suggesting prominent roles of SRB in Hg(II) methylation. Without the addition of sulfate in the bog soil or when sulfate was depleted in the fen soil (after 15 days), both SRB and methanogens contributed to MeHg production. Analysis of microbial community composition confirmed the presence of several phyla known to harbor microorganisms associated with Hg(II) methylation in the soils. These observations suggest that SRB and methanogens were mainly responsible for Hg(II) methylation in these tundra soils, although their relative contributions depended on the availability of sulfate and possibly syntrophic metabolisms between SRB and methanogens.

Key words: Mercury, methylation, acetate, sulfate, microbial community, syntrophy

1. Introduction

Arctic tundra soil stores a globally significant amount of mercury (Hg) due to atmospheric deposition and a high content of soil organic matter that has a high binding affinity for Hg (Obrist et al., 2017; Schuster et al., 2018). The greatest toxicological concern of Hg pollution is the transformation of inorganic mercuric Hg(II) to methylmercury (MeHg), which is a potent neurotoxin that bioaccumulates and biomagnifies through food webs in the Arctic ecosystem. Production of MeHg has been reported in Arctic wetland ponds, lake sediments, and tundra soils (Barkay and Poulain, 2007; Lehnherr et al., 2012; Schartup et al., 2015; Yang et al., 2016a), which are important sources of MeHg in Arctic freshwater and the Arctic Ocean (Kirk et al., 2012; Lehnherr, 2014; Schartup et al., 2015). However, our current understanding of the biogeochemical drivers of Hg(II) methylation is limited in tundra soils. Recent studies reported that warming increased MeHg production in these soils, possibly through enhanced degradation of soil organic carbon (SOC) that releases low molecular weight (LMW) labile organic carbon and nutrients (e.g., acetate, phosphorus, and nitrogen) and fuels microbial production of MeHg (MacMillan et al., 2015; Yang et al., 2016a). LMW labile organic carbon compounds, such as acetate, are important substrates and can be consumed in anaerobic biogeochemical processes of methanogenesis, ferric iron [Fe(III)] reduction, and sulfate reduction. Net accumulation of acetate has been found in the top organic soil layer but net consumption was found in the lower mineral soil layer after incubation at 8 °C (Yang et al., 2016a). The LMW labile organic carbon could also be transported into a deeper mineral layer through vertical movement or mixing due to cryoturbation between the organic and mineral layer soils (Drake et al., 2015; Yang et al., 2016b). Although correlations between MeHg production and labile organic carbon mineralization have been suggested

(MacMillan et al., 2015; Yang et al., 2016a), the roles of LMW organic acids (e.g., acetate) in microbial Hg(II) methylation remain unclear in the Arctic tundra soils.

Moreover, it remains elusive about who are the dominant Hg(II) methylators in these Arctic soils. MeHg is produced by a small group of anaerobic microorganisms carrying a two-gene cluster *hgcAB* essential for Hg(II) methylation (Parks et al., 2013). These microbes may include, but are not limited to, sulfate-reducing bacteria (SRB), iron-reducing bacteria (FeRB), methanogens, and fermenters (Bravo et al., 2018; Gilmour et al., 2013; Jones et al., 2020; Liu et al., 2018; Yu et al., 2013), although their contributions to MeHg production vary with geochemical conditions in different environmental systems. Several studies reported that methanogens and FeRB were dominant members of Hg(II) methylating community in rice paddy soils and in boreal lakes (Bravo et al., 2018; Liu et al., 2018), while others found that SRB were the principal Hg(II) methylators in some freshwater sediments or boreal wetlands (Jones et al., 2020; Schaefer et al., 2020). In the high Arctic wetlands, one study suggested that SRB were not the major Hg(II) methylators due to a low prevalence of SRB (Loseto et al., 2004), while others proposed that SRB could be active in these soils (Barkay and Poulain, 2007). A laboratory incubation study of Arctic tundra soils found no significant correlations between Hg(II) methylation and sulfate reduction because of low sulfate concentrations (Yang et al., 2016a). However, sulfate concentrations can vary greatly among these soils through precipitation or seawater intrusion (Mitchell et al., 2008; Tully et al., 2019). High sulfate concentrations may stimulate the growth and activity of SRB and promote MeHg production (Gilmour et al., 1992; Jones et al., 2020; Mitchell et al., 2008; St. Pierre et al., 2014), but other studies reported that sulfate addition may not affect Hg(II) methylation as SRB and related syntrophs may instead metabolize alternative substrates via syntrophic fermentation of organic compounds with methanogens (Schaefer et al., 2020). While methanogens and FeRB play

important roles in coupled activities of SOC transformation, methanogenesis, and Fe(III) reduction (Woodcroft et al., 2018; Yang et al., 2017), their contributions to Hg(II) methylation in Arctic tundra soils are unclear. A better understanding is thus needed to determine who are the principal Hg(II) methylators in the Arctic tundra soils, and whether these methylators are site-specific and how they are related to geochemical characteristics of the soils.

In this study, we conducted laboratory microcosm incubation experiments to investigate microbial production of MeHg in two contrasting Arctic tundra soils: a circumneutral fen soil from the toe of a hillslope and an acidic bog soil, both collected near Nome, Alaska, United States. Our main objectives were to determine (1) how an increase in the availability of substrates, acetate and sulfate, may affect MeHg production, and (2) who are the dominant Hg(II) methylators. We hypothesize that suppression of SRB and methanogens by their respective inhibitors, molybdate and 2-bromoethanesulfonate, could slow down or cease MeHg production in the tundra soils. This hypothesis was tested by a series of incubation experiments in the presence or absence of various substrates and/or microbial inhibitors and by 16S rRNA gene sequence analyses to tease out major microbial compositions and changes during incubation.

2. Materials and Methods

2.1. Study site and characterization of soil samples

Active-layer soil cores were collected during an August 2018 field campaign from the Intensive Site 9 (fen) near Teller Road Mile 27 (64.729193°N, 165.944072°W) and from a thermokarst depression (bog) at the Council Road Mile 71 site (64.859618°N, 163.703477°W) in Alaska, United States, as part of the Next Generation Ecosystem Experiment (NGEE-Arctic)

(Philben et al., 2020). For the clarity of the presentation and comparisons, herein we refer the Teller soil as the "fen" soil, and the Council soil as the "bog" soil. The Teller site is characterized by a 130-m elevation gradient and a diverse vegetation cover, including tall shrubs, dwarf shrubs, mosses, and graminoids and a water table at or near the soil surface (Léger et al., 2019; Philben et al., 2020). The soil layer consists of an organic rich upper part and shows a gradual increase in bulk density with depth. The National Ocean and Atmospheric Administration's (NOAA's) meteorological station at Nome Airport indicates that over a 5-year average (2013 to 2017) the mean annual air temperature is –1.02 °C, the yearly rain precipitation is 450.6 mm, and the yearly snowfall is 1704.8 mm (Léger et al., 2019). The Council site is composed of mostly moist acidic tussock tundra, and the dominant vegetation is cotton grass (*Eriophorum vaginatum*) or tussock, blueberry (*Vaccinium uliginosum*), and lichen and moss (*Sphagnum* spp.) beds. The mean annual air temperature is –2.1 °C, and the annual precipitation is about 485 mm (Kim et al., 2016). Following the collection of soil cores (~5 cm in diameter and 20 cm in depth), they were sealed in Whirl-Pak bags, and stored at –22 °C until use. Soil porewater was also collected from the subsurface of the sites by piezometers and MacroRhizons, and stored for analyses of pH and dissolved methane (CH_4) (described in Section 2.3.).

Soil water contents (Table 1) were determined by oven-drying the pre-weighed wet soil at 60 °C until a constant mass was obtained and then calculating the mass difference before and after drying normalized to the initial wet weight [i.e., (wet weight–dry weight)/(wet weight)×100%]. Sequential extraction of the soils was conducted to determine extractable Hg pools using a modified method from previous studies (Bloom et al., 2003; Lu et al., 2019; Miller et al., 2013). The soils were extracted sequentially with (1) 0.01 M HCl and 0.1 M CH_3COOH (F1), (2) 1 M KOH (F2), and (3) a mixture of concentrated HCl and HNO_3 (aqua regia) at a volumetric ratio of

10:3 (F3). These pools of Hg were operationally defined as acid-soluble Hg (F1), organo-chelated Hg (F2), and mercuric sulfide (HgS) Hg (F3) (Bloom et al., 2003; Lu et al., 2019; Miller et al., 2013). Briefly, a subsample of the homogenized wet soil (~0.5 g) was equilibrated with 20 mL of the extractant F1 on an end-to-end rotary shaker (120 rpm) for 18±4 h. The soil suspension was then centrifuged at 2000×*g* for 15 min, and the supernatant filtered through 0.2-μm filters to collect the filtrate. This step was repeated by mixing the soil pellet after centrifugation with another 20 mL of the extractant F1, and the filtrate was again collected and combined with above filtrate. The remaining soil pellet was added with 20 mL of the extractant F2, and the same extraction procedure was used to extract organo-chelated Hg. Lastly, 13 mL aqua regia (F3) was added to the soil pellet after F2 extraction for overnight digestion, and then diluted with Milli-Q water to a final volume of 40 mL. Total Hg was extracted directly by digesting an aliquot of 0.5–1 g wet soil in 13 mL aqua regia overnight and then diluting it to 40 mL with Milli-Q water. The extractant solutions were finally oxidized with BrCl (0.5% v/v) and stored at 4 °C overnight or longer until analyses, as previously described (Miller et al., 2009; Zhang et al., 2021).

2.2. Soil microcosm incubations

Soil microcosm experiments were the same as those reported in a recent study focusing on greenhouse gas production and anaerobic respiration pathways of soil organic carbon (Philben et al., 2020), while the present study focused on Hg(II) transformation. Briefly, soil cores were thawed and homogenized inside an anoxic glove bag (Coy Lab Products, Grass Lake, MI) under ~98% N_2 and 2% H_2 atmosphere. The homogenized wet soil (3.0±0.1 g) from each site was transferred into a series of autoclaved serum bottles (26 mL) in the glove bag. Molybdate and 2-bromoethanesulfonate (BES) were used as selective inhibitors of SRB and methanogens, respectively, as previously described (Hamelin et al., 2011; Kronberg et al., 2018; Schaefer et al.,

2020). The soil was thoroughly mixed and then incubated following the addition of 0.2 mL each of the amendments: (1) degassed Milli-Q wssater (unamended control); (2) sodium acetate (acetate); (3) sodium acetate and BES (acetate+BES); (4) sodium acetate and sodium molybdate (acetate+Mo); and (5) ^{202}Hg-enriched Me^{202}Hg (Olsen et al., 2016). The added concentrations of acetate, BES, molybdate, and Me^{202}Hg were 9.2, 7.1, 1.4 μmol, and 0.3 ng g^{-1} wet soil, respectively (Appendix A Table S1). Since the two soils differed in water contents (Table 1), the final amendment concentrations per g dry weight were also provided in Appendix A Table S2. Additionally, due to a low sulfate concentration in the bog soil, a sixth amendment with sulfate (at ~13.3 μmol g^{-1} wet soil) was performed to investigate the effects of increasing sulfate availability on MeHg production. All the serum bottles were then capped with thick rubber stoppers, sealed with aluminum crimps, and flushed with ultra-pure N_2 for 10 min. Three replicates were constructed for each treatment at each sampling timepoint. Note that inhibitor experiments with the fen soil (Amendments 3 and 4) were monitored up to 30 days due to limited availability of the soil, and all others were monitored up to 60 days. An incubation temperature of 8 °C was used to simulate relatively high temperatures observed in summer months for accelerated microbial methylation (Kim et al., 2016; Léger et al., 2019), although the average mean annual air temperatures are about –1.0 to –2.1 °C at these sites. Changes in ambient MeHg and Me^{202}Hg concentrations over the course of incubation were measured separately to determine respective methylation and demethylation in the soil.

2.3. Chemicals and chemical analyses

All chemicals used in this study are certified analytical reagents from Sigma-Aldrich and Fisher Scientific, and no detectable amounts of Hg were found in the stock solution of these reagents, as previously reported (Wang et al., 2020). Enriched Hg stable isotopes, ^{202}Hg (95.86%) and ^{200}Hg

(96.41%), were obtained from the Isotope Enrichment Program at the Oak Ridge National Laboratory, Oak Ridge, Tennessee, United States (Zhang et al., 2021), and used for the synthesis of isotopically labeled MeHg using the previously established method (Hintelmann and Ogrinc, 2002; Parks et al., 2013).

Dissolved CH_4 concentrations in soil porewater (collected in sealed serum bottles in the field) were determined by equilibrating 1 mL porewater in crimp-sealed serum vials and then analyzing the headspace CH_4 using a gas chromatograph (GC) equipped with a methanizer and a flame ionization detector (SRI 8610C, SRI Instruments, Torrance, CA). The final CH_4 concentration was calculated based on Henry's law, as described previously (Philben et al., 2019). Similarly, headspace concentrations of CH_4 and CO_4 in the incubation bottles were analyzed at predetermined time intervals.

Following gas measurement, triplicate soil microcosms were destructively sampled. An aliquot of the soil (0.5–1 g wet weight) was digested in 10 mL of 1.5 M KBr in 5% H_2SO_4 and 2 mL of 1 M $CuSO_4$ for 1 h to release MeHg from the sample matrix as bromide derivatives by the combined reaction of KBr and Cu^{2+} under acidic pH conditions (Alli et al., 1994; Furutani and Rudd, 1980). This was followed by the addition of 10 mL methylene chloride (99.99%, Fisher Scientific) for an additional 1 h to extract MeHg (Bloom et al., 1997; Yang et al., 2016a). $Me^{200}Hg$ was added to each sample as an internal standard to correct potential interferences or loss of MeHg during extraction and subsequent distillation processes. MeHg was then determined using a modified EPA Method 1630 via distillation, ethylation, trapping, and thermo-desorption with an automated MERX purge and trap system (Brooks Rand, Seattle, WA), followed by separation by gas chromatography, decomposition through a pyrolytic column, and detection on an inductively coupled plasma mass spectrometer (ICP-MS) (Elan DRC-e, PerkinElmer, Shelton, CT) (Zhang et

al., 2021). A sediment reference material (ERM-CC580 with a certified value of 75±4 ng MeHg g^{-1}) was extracted and run in parallel with samples for quality assurance and quality control (QA/QC). The measured values of the reference material ranged from 69.5 to 80.2 ng/g, and the recovery was within 100±10%. Calibration verification samples with known amounts (50 pg) of ambient MeHg (a reference standard from Brooks Rand) and $Me^{202}Hg$ (25 pg) were also run about every 20 samples with a mean recovery of 100±3.5% (Zaporski et al., 2020; Zhang et al., 2021). The detection limit for MeHg on ICP-MS was about 6 pg Hg, equivalent to a detection limit of ~ 0.02 ng Hg g^{-1} dw soil. For inorganic Hg(II) analysis, the extractant solutions after sequential extraction (Section 2.1) were reduced with $SnCl_2$ (100 mM), followed by purging with high-purity N_2 and detection of purgeable elemental Hg(0) on a Zeeman cold vapor atomic absorption spectrometer (CVAAS) (Lumex RA-915+, Ohio Lumex Co.). Hg calibration standards (0, 25, 50, 75, 100 pg) were also run with the samples, and the detection limit of Hg by CVAAS was about 10 pg (Lu et al., 2019).

Another two aliquots of the remaining soil (0.75 g wet wt) were extracted with 10 mL of degassed Milli-Q water or 0.1 M KCl. The soil slurry was shaken for 1.5 h and centrifuged at 3000×*g*, and the supernatant was collected by filtering through a 0.2-μm PTFE syringe filter. The KCl extracts were immediately used to determine pH and ferrous Fe(II) concentrations with 1,10-phenanthroline (Hach method 8146) using a portable colorimeter (Hach DR900 Colorimeter) (Philben et al., 2019; Yang et al., 2016b). The detection limit was ~0.25 μmol Fe g^{-1} dw. All water extract samples were analyzed within three days of collection or frozen at –23 °C until analysis. Major anions (e.g., SO_4^{2-} and NO_3^-) and organic acids (e.g., formate, acetate, and propionate) were analyzed using previously established methods (Philben et al., 2019; Yang et al., 2016b). They were separated on a Dionex AS15 analytical column and an AG15 guard column and analyzed by

an ion chromatograph (Dionex Integrion, Thermo Scientific) equipped with a conductivity detector. The detection limit for each anion and organic acid was ~0.14 μmol g^{-1} dw. WEOC was measured on a total organic carbon analyzer (TOC, Shimadzu) after the samples were acidified in 0.1% HCl and purged to remove inorganic carbonates (Philben et al., 2019; Yang et al., 2016b), and the detection limit was ~0.31 μmol C g^{-1} dw. For statistical analyses, all data were validated for normality using Shapiro-Wilk test (Schwartz et al., 2019). Differences in Hg species distributions between the two soils were tested by the two-sample t-test. Multi-comparisons of MeHg concentrations among samples with different amendments at day 15 or day 30 were tested by analysis of variance (ANOVA) and pairwise comparisons (Bonferroni test), using the OriginPro analysis software (OriginLab, Northampton, MA) with a significance threshold of P=0.05.

2.4. Soil DNA extraction and 16S rRNA amplification

Soil DNA extractions were performed in triplicate from pre-incubation bulk samples (n=3 technical replicates) and the incubated samples (n=3 per sampling point per treatment). We analyzed a total of 86 samples generated through incubations from the fen and bog soils (Philben et al., 2020). Total DNA was extracted by using 0.25 g of wet soil as input to the DNeasy PowerSoil Kit (Qiagen, Germantown, MD, USA), where the samples were incubated in bead-solution at 65 °C for 5 min prior to bead-beating. Samples were disrupted by bead beating with a 1600 MiniG (SPEX Sample Prep, Metuchen, NJ, USA) at a setting of 1500 RPM for 60 s, and the DNA was further purified according to the kit protocol. 16S rRNA genes were amplified by PCR using primers (F515/R806) that target the V4 region of the 16S rRNA gene where the reverse PCR primer was barcoded with a 12-base Golay code (Caporaso et al., 2011). These primers contained degeneracy added to both the forward and reverse primers and were not biased in detecting methanogenic Archaea, hence used to perform concurrent analysis of bacteria and archaea in the

252 samples. The PCR reactions were performed as described previously (Philben et al., 2020). Each
253 sample was amplified in triplicate, combined, purified with Agencourt AMPure XP PCR
254 purification system (Beckman Coulter, Brea, CA), and quantified using the Qubit dsDNA HS
255 assay (Invitrogen, Carlsbad, CA, USA). Amplicons were pooled (10 ng/sample) and sequenced on
256 one lane of the Illumina Miseq platform (Illumina Inc, San Diego, CA). Quality filtered sequence
257 data were deposited at European Nucleotide Archive (PRJEB37429).

258 *2.5. 16S rRNA gene sequence analysis*

259 Paired-end amplicon sequences were overlapped and merged using FLASH (Magoč and
260 Salzberg, 2011). Quality filtering (>q30) and demultiplexing (Bokulich et al., 2013) resulted in
261 445,195 sequences for the fen soil and 327,007 sequences for the bog soil. Sequences were grouped
262 into operational taxonomic units (OTUs) based on 97% sequence identity, and chimeric sequences
263 were removed using UPARSE (Edgar, 2013). OTUs were given taxonomic assignments in QIIME
264 (Caporaso et al., 2010) version 1.7.0 using the RDP classifier (Wang et al., 2007) and the SILVA
265 database 132 (Quast et al., 2012). Phylogenetic trees were created using FastTree (Price et al.,
266 2010) under QIIME's default parameters. All remaining analyses were performed in R version
267 3.5.1 (Bates et al., 2014; Team, 2013) via use of phyloseq (McMurdie and Holmes, 2013), taxize
268 (Chamberlain and Szöcs, 2013), vegan (Oksanen et al., 2013), and ggstatsplot (Patil, 2019)
269 packages. Amplicon data were proportionally rarified (to the 90% of the minimum sample depth
270 in the dataset without replacement resulting in 7000 sequences per sample) and normalized, and
271 β-diversity (Shannon's H) was assessed using Bray-Curtis distance (Bray and Curtis, 1957). For
272 multiple comparisons, *P* values were adjusted via Bonferroni method. Strains and taxa associated
273 with Hg(II) methylation based on the presence of the marker gene *hgcA* were retrieved from the
274 Integrated Microbial Genomes & Microbiomes (IMG/M) database of the Joint Genome Institute

(JGI). The sequence of *hgcA* from the well characterized methylator *Desulfovibrio desulfuricans* ND132 (locus tag DND132_1056, IMG Gene ID 2503785873) was used as the query gene for the Homolog Toolkit in IMG/ER, which uses the Basic Local Alignment Search Tool (BLAST) with an e-value cutoff of 1×10^{-5} to identify homologs present in IMG. Homologous sequences without the conserved sequence motif [G(I/V)NVWC(A/S/G)(A/S/G)GK] were removed (Cooper et al., 2020; Parks et al., 2013), which resulted in 604 unique genomes with confirmed *hgcA* genes (Appendix B). Full taxonomic lineages for the identified *hgcA* genomes were retrieved using the taxize package (Chamberlain and Szöcs, 2013). The results were compared to 16S rRNA sequencing results to select taxa that may harbor mercury methylating bacteria.

3. Results and Discussion

3.1. Geochemical properties of the fen and bog soils

Geochemical properties of the fen and bog soils are shown in Table 1. Notably, the bog soil was more acidic, with a pH of 5.2±0.2, than the fen soil, with a pH of 6.7±0.2 (Table 1). The dissolved CH_4 concentration was lower in the porewater in the fen soil (0.04±0.002 mM) than in the bog soil (0.36±0.04 mM). The total C contents were 26% and 17% in the fen and bog soils, respectively. Consistently, WEOC in the fen soil extract [50.0±22.0 μmol g^{-1} dry weight (dw) soil] was higher than that in the bog soil (31.7±2.0 μmol g^{-1} dw). The total extractable LMW organic acids (2.38±0.07 μmol g^{-1} dw) in the fen soil were about twice of those in the bog soil (1.22±0.06 μmol g^{-1} dw). Extractable Fe(II) and sulfate concentrations were 5.4±0.2 μmol g^{-1} dw and <0.14 μmol g^{-1} dw (or below the detection limit), respectively, in the bog soil, and were 2.7±0.2 μmol g^{-1} dw and 0.45±0.04 μmol g^{-1} dw in the fen soil (Table 1). These observations suggest that the bog

soil was likely more reducing than the fen soil, as the water table at the Teller fen site is more fluctuating due to runoff along the hillslope (Philben et al., 2020).

Table 1. Comparisons of field porewater and soil extract properties of the fen and bog soils

Field properties	Fen	Bog[c]
pH of field porewater	6.7±0.2[a]	5.2±0.2*
Dissolved CH_4 in porewater (mM)	0.040±0.002	0.36±0.04**
Water content (%)	71±0.1	62±0.2*
Total C (%)	26±0.3	17±0.2*
Soil extract properties		
pH	6.7±0.2	5.2±0.2*
Sulfate (μmol g^{-1} dw)	0.45±0.04	<0.14**
Fe(II) (μmol g^{-1} dw)	2.7±0.2	5.4±0.2*
WEOC[b] (μmol g^{-1} dw)	50.0±22.0	31.7±2.0
Sum of organic acids (μmol g^{-1} dw)	2.40±0.07	1.20±0.06*
THg (ng g^{-1} dw)	63.6±4.5	34.6±2.0*
MeHg (ng g^{-1} dw)	0.11±0.01	0.86±0.05**

Notes: a. Data averaged from triplicate samples with errors representing one standard deviation.
b. WEOC = water-extractable organic carbon; THg = total mercury.
c. Significant differences between the two soils are marked as (*) $P<0.05$ and (**) $P<0.01$.

Sequential extraction results showed similar patterns of extractable Hg pools in both the fen and bog soils (Fig. 1). The acid-soluble Hg accounted only for about 0.24% of the total Hg in both soils. The HgS-like pool accounted for ~22% and 17.8% in the fen and bog soils, respectively. However, the majority of Hg in the tundra soils was associated with soil organic matter (Fig. 1), resulting from its high binding affinities with Hg (Lehnherr, 2014; Zhang et al., 2019). The fen soil showed ~77.7% organo-chelated Hg and the bog soil ~82%, and no significant differences in Hg species distributions were observed between the two soils. Interestingly, although the total Hg (THg) in the bog soil (34.6±2.0 ng g^{-1} dw) was only ~54% of that in the fen soil (63.6±4.5 ng g^{-1} dw), the MeHg concentration in the bog soil (0.86±0.05 ng g^{-1} dw) was about 7-fold higher than

318 that in the fen soil (0.11±0.004 ng g^{-1} dw). The higher total Hg but lower MeHg concentrations in
319 the fen soil than the bog soil imply that differences in soil hydrobiogeochemical conditions may
320 have influenced net Hg(II) methylation. More specifically, the more stagnant, reducing
321 environments in the bog soil likely favored MeHg production by anaerobic microorganisms (Parks
322 et al., 2013; Podar et al., 2015), as compared to the hillslope fen soil with frequent water table
323 fluctuations and runoffs (Philben et al., 2020).

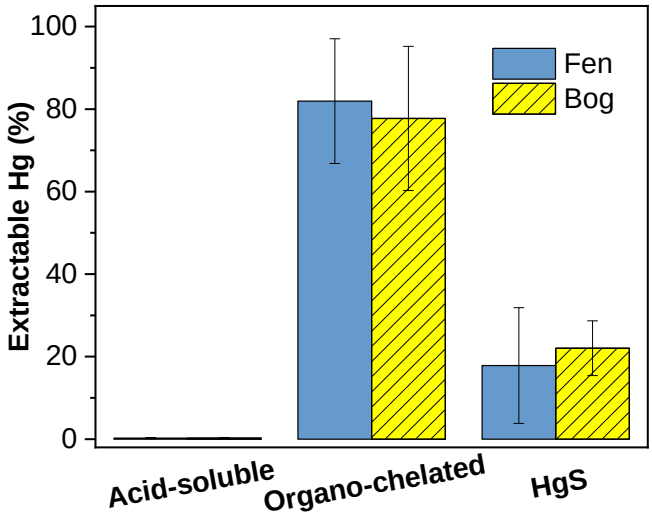

324

325 **Fig. 1.** Sequential extraction of Hg in the fen and bog soils. Three Hg pools were extracted and
326 defined as: (1) acid-soluble Hg extracted by 0.01 M HCl and 0.1 M CH_3COOH, (2) organo-
327 chelated Hg extracted by 1 M KOH, and (3) HgS extracted by aqua regia. Data were averaged
328 from triplicate samples with error bars representing one standard deviation. Each extractable Hg
329 pool was normalized to the measured total Hg in the fen soil (63.6±4.5 ng g^{-1} dw) or in the bog
330 soil (34.6±2.0 ng g^{-1} dw). No significant changes were observed in each Hg pools between the two
331 soils at P= 0.05.

332 *3.2. Methylmercury production in the fen soil*

333 Microcosm incubations resulted in a rapid increase in MeHg production in the
334 circumneutral fen soil, particularly in the first 30 days either with or without (unamended) acetate

addition (Fig. 2a). The MeHg concentration in the unamended soil increased from 0.11±0.004 at day 0 to 0.36±0.02 ng g^{-1} dw at day 30 (Fig. 2a). However, after 30 days, MeHg production slowed down, and its cumulative concentration increased to only ~0.39±0.06 ng g^{-1} dw from day 30 to 60. The incubation with acetate addition produced similar amounts of MeHg as in the unamended soil (Fig. 2a), indicating that increasing acetate concentration had little effect on MeHg production or accumulation in the fen soil.

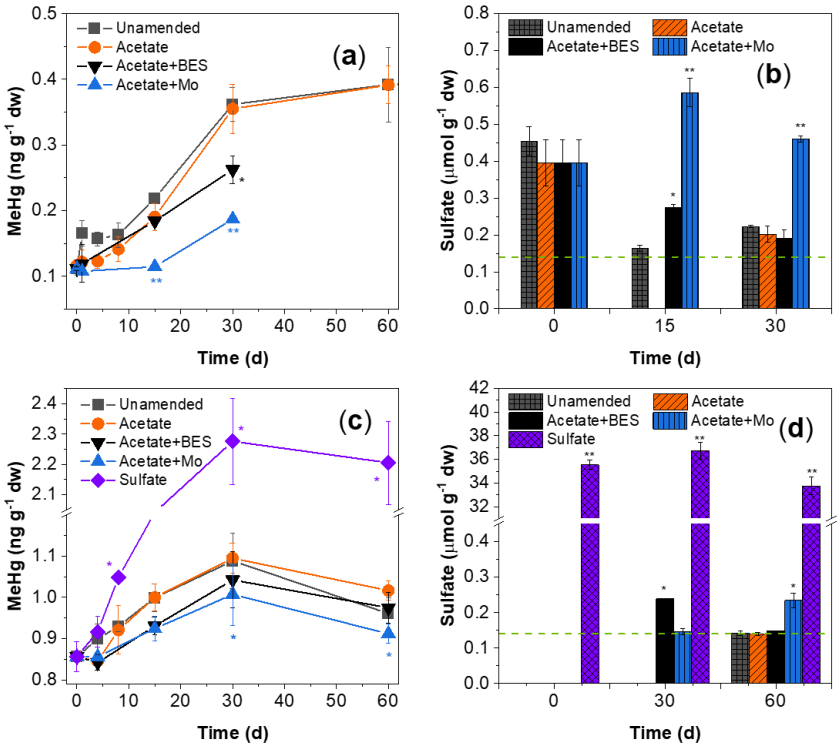

Fig. 2. Effects of acetate addition and microbial inhibitors on MeHg production and water-extractable sulfate concentrations in the fen (**a, b**) and bog (**c, d**) soils at 8 °C. Data were averaged from triplicate incubations with error bars representing one standard deviation. Sulfate concentrations (Philben et al., 2020) below the detection limit (indicated by dotted lines) are not shown. Significant changes among treatment groups at each timepoint are marked as (*) $P<0.05$ and (**) $P<0.01$. Inhibitor-addition incubations of the fen soil were not conducted at day 60.

Experiments with selective microbial inhibitors showed that the addition of BES did not significantly affect MeHg production in the fen soil within the first 15 days (Fig. 2a), as a similar amount of MeHg (0.18±0.01 ng g^{-1} dw) was observed as those in the control incubations (unamended and acetate-amended treatments) (P=1). The result suggests that methanogens played a negligible role in MeHg production, as BES is a structural analog of coenzyme M (CoM) and a competitive inhibitor of methyl-CoM reductase enzyme required for methanogenesis (Hamelin et al., 2011; Kronberg et al., 2018; Schaefer et al., 2020). In contrast, molybdate addition nearly halted Hg(II) methylation in the first 15 days and no net increase in MeHg production was observed from day 0 to day 15 (P<0.001) (Fig. 2a). Consistent with the pattern of MeHg production, addition of molybdate inhibited sulfate reduction, as molybdate is known to inhibit SRB by mechanisms including inhibition of the key ATP sulfurylase enzyme and interference with sulfate transport (Biswas et al., 2009). Therefore, the sulfate concentration increased, rather than decreased, within the first 15 days (Fig. 2b). This increase in sulfate concentrations in the acetate+molybdate treatment at days 15 and 30 was attributed to both the lack of microbial reduction and the addition of a relatively high concentration of acetate (31.7 μmol g^{-1} dw) and molybdate (4.8 μmol g^{-1} dw) resulting in desorption or anion exchange of sulfate initially adsorbed on the soil (Antelo et al., 2012; Philben et al., 2020). In contrast, water-extractable sulfate concentrations in all other treatments decreased from ~0.4 μmol g^{-1} dw at day 0 to near or below the detection limit (~0.14 μmol g^{-1} dw) after 15 days, indicating active sulfate reduction. Evidently, the halted Hg(II) methylation in the molybdate-amended soil was well correlated to suppressed sulfate reduction or microbial activities of SRB by molybdate. These results suggest that SRB likely played a dominant role in Hg(II) methylation whereas methanogens played a negligible role in the first 15 days.

The inhibition patterns of BES and molybdate on MeHg production, however, varied after 15 days when sulfate became depleted (Fig. 2a). From day 15 to day 30, while the addition of molybdate still inhibited MeHg production, it did not completely halt Hg(II) methylation as observed within the first 15 days, and MeHg concentration increased from 0.11±0.003 ng g^{-1} dw at day 15 to 0.19±0.003 ng g^{-1} dw at day 30 in the molybdate-amended incubation. The amount of MeHg accumulation (0.08±0.01 ng g^{-1} dw) was only 33.3±5.4% of that observed in the control incubation (0.24±0.025 ng g^{-1} dw), implying that SRB potentially contributed up to ~67% to Hg(II) methylation. Coincidentally, MeHg production in the BES-amended incubation was ~38% lower than that in the control experiment at day 30 (Fig. 2a), suggesting that methanogens contributed up to ~38% of the methylation. Therefore, both SRB and methanogens appeared to be the major contributors to Hg(II) methylation after 15 days when sulfate was consumed in the incubations without molybdate or BES additions (Fig. 2b). SRB thus could be inhibited and unable to outcompete methanogens (Dang et al., 2019; Hausmann et al., 2016). Instead, SRB might form syntrophic partnerships with methanogens (Yu et al., 2018), and both clades could contribute to Hg(II) methylation. These observations are consistent with recent work reporting concomitant SRB and methanogen activities in methylating Hg(II) in boreal wetlands (Schaefer et al., 2020). It was found that, in the absence of sulfate and other electron acceptors, SRB syntrophs could act as fermenters and transfer electrons to methanogens, thereby increasing MeHg production (Yu et al., 2018). Inhibition of either one of the microbial groups may thus suppress MeHg production (Schaefer et al., 2020). Therefore, there appears a transition of responsible microbial communities from predominantly SRB in the first 15 days to both SRB and methanogens after 15 days in methylating Hg(II), and this transition was affected by geochemical properties of the soil or the availability of sulfate.

3.3. Methylmercury production in the bog soil and comparisons with the fen soil

In the acidic bog soil, rapid MeHg production was also observed either with or without the addition of acetate during incubation (Fig. 2c). The MeHg concentration in the unamended incubation increased from 0.86±0.05 ng g^{-1} dw at day 0 to 1.09±0.07 ng g^{-1} dw at day 30 (Fig. 2c), which was comparable to the amount of MeHg increased in the Teller fen soil. After 30 days, MeHg amount reached a plateau and even decreased in some incubations at day 60, especially in the unamended and acetate-only-amended incubations. The addition of acetate again showed negligible effects on MeHg production, as similar concentrations of MeHg were observed in the unamended and acetate-only-amended bog soil treatments (P=1) (Fig. 2c). These results suggest that the observed slower MeHg accumulation in both the fen and bog soils after 30 days of incubation (Figs. 2a and 2c) could not be attributed to limited availability of labile organic C. Moreover, acetate concentration declined (~10 μmol g^{-1} dw) in the acetate-only-treated fen soil (Appendix A Fig. S1b), but no consumption of acetate was observed in the bog soil (Appendix A Fig. S2b). Hence, MeHg accumulation did not correlate with acetate consumption. These observations are consistent with a previous study showing that acetate addition did not affect MeHg production in peatlands, which also contained high amounts of labile organic C (Mitchell et al., 2008). However, our results differ from a recent study reporting that acetate addition substantially increased MeHg production in sand dune sediments (Zaporski et al., 2020). These different findings may be attributed to a much lower availability of labile C substrates in the sand dune sediments than that in the tundra soils. The sand dune sediments contained low concentrations of acetate (<0.1 μmol g^{-1} dw) and WEOC (1.5 μmol g^{-1} dw) (Zaporski et al., 2020), while the tundra soils used in this study contained much higher amounts of acetate (0.8~1.7 μmol g^{-1} dw) and WEOC (>30 μmol g^{-1} dw) (Table 1). Therefore, the availability of abundant organic C

substrates did not limit microbial activities in methylating a small quantity of Hg(II) in both the fen and bog soils, so that increasing acetate availability showed insignificant effects on MeHg production.

With exception of the sulfate-amended treatment, there were no clear trends of sulfate reduction observed in all the incubations of the bog soil (Fig. 2d), in part due to its low sulfate concentrations (Fig. 2d, Table 1). However, the addition of sulfate to the bog soil substantially promoted MeHg production as compared to those without sulfate amendment (Fig. 2c), suggesting that sulfate was a limiting factor of Hg(II) methylation in this soil. At day 30, net MeHg production in the sulfate-amended incubation was 1.42±0.14 ng g^{-1} dw, about 5-fold higher than those observed in the no-sulfate-amended incubations. The result suggests that Hg(II) methylation was strongly influenced by sulfate reduction in the soil. However, between day 30 and 60, MeHg production in the sulfate-amended incubation slowed down or decreased, similarly as observed in the fen soil, although the sulfate concentration remained high after 60 days (~33.7 μmol g^{-1} dw) (Fig. 2d). The decrease in MeHg concentrations could be partially attributed to potential demethylation in the soil, as previously reported (Barkay and Gu, 2021; Bridou et al., 2011; Hamelin et al., 2015; Lu et al., 2017). This conclusion is supported by additional experiments incubating both the fen and bog soils with isotopically labeled $Me^{202}Hg$. The results showed an insignificant decrease in $Me^{202}Hg$ concentrations at day 30 in both soils (Appendix A Fig. S3). However, at day 60, the $Me^{202}Hg$ concentration decreased significantly (P=0.028) in the bog soil. Therefore, the plateaued or decreased MeHg concentrations during incubation could be attributed to concurrent methylation and demethylation, although additional biogeochemical factors, such as the formation of HgS, bioavailable Hg(II) pools, and electron acceptors, may also limit MeHg production in these soils (Lin et al., 2014; Luo et al., 2017; Mitchell et al., 2008).

The effects of BES and molybdate inhibitors on Hg(II) methylation differed between the bog and fen soils. Unlike the fen soil, the addition of BES or molybdate only partially inhibited MeHg production (differences insignificant at $P=0.05$) in the first 15 days in the bog soil (Fig. 2c). At day 15, the average amounts of MeHg produced in the BES-amended and molybdate-amended soils were 0.076±0.042 and 0.069±0.047 ng g^{-1} dw, respectively, equivalent to about 52.8±33.6% and 47.5±37.9% of MeHg produced in the controls (i.e., 0.15±0.05 ng g^{-1} dw in the unamended and acetate-only-amended soils). This inhibition pattern did not change over time, suggesting that both SRB and methanogens continuously contributed to Hg(II) methylation in the bog soil. The effectiveness of molybdate and BES in inhibiting SRB and methanogens was evident in substantially decreased sulfate reduction (Appendix A Figs. S1 and S2) or stalled CH_4 production (Appendix A Fig. S4) over the incubation period.

Together, these results indicate that Hg(II) methylation was not limited by acetate, likely due to its high abundance in the fen and bog soils. However, sulfate availability is an important factor in affecting SRB activity for MeHg production in these tundra soils. Comparing the incubation results between the fen and bog soils, SRB appeared to play a dominant role in MeHg production via sulfate reduction when sulfate was available (e.g., in the first 15 days of incubation of the fen soil) (Fig. 2a). In the sulfate-deficient bog soil, sulfate amendment therefore substantially increased MeHg production (Fig. 2c). However, when sulfate availability was limited, similar inhibition patterns by BES and molybdate on MeHg production were observed in the fen soil after 15 days (Fig. 2a) and in the bog soil (Fig. 2c), suggesting a potential role of SRB-methanogen syntrophic partnerships in Hg(II) methylation, as previously reported (Schaefer et al., 2020; Yu et al., 2018). While it is difficult to pinpoint whether both SRB and methanogens or only one of them were methylating Hg(II) as MeHg production could be suppressed by inhibition of either one of

the metabolic groups (Schaefer et al., 2020), both methanogens and SRB at least directly or indirectly contributed to MeHg production in these tundra soils (see additional details in Section 3.4 and 3.5). For a long time, the role of SRB in Hg(II) methylation in tundra soils have been controversial, likely due to low sulfate concentrations or low SRB activities in these soils (Barkay and Poulain, 2007; Loseto et al., 2004; Yang et al., 2016a). Our results indicate that SRB abundance and activities could be stimulated by increasing sulfate concentrations and thus play an important role in biogeochemical transformation of Hg(II) in these soils (Åkerblom et al., 2020; Hu et al., 2020; Mitchell et al., 2008). Moreover, even when sulfate is limiting, SRB could potentially develop syntrophic partnership metabolizing alternative substrates with methanogens (Plugge et al., 2011), thereby contributing to MeHg production. Depending on sulfate availabilities in the fen and bog soils, SRB could contribute about 50%–100% directly or indirectly to MeHg production. However, we cannot rule out that other microbes may have contributed to Hg(II) methylation. Nitrate concentrations did not change appreciably over the incubation in both soils (Philben et al., 2020), suggesting that denitrifiers were not involved in Hg(II) methylation in these soils. FeRB may contribute to MeHg production (discussed in Section 3.5), as active Fe(III) reduction was observed in both the fen and bog soils during incubation (Philben et al., 2020). However, there are no specific inhibitors for FeRB (Bravo et al., 2018; Schaefer et al., 2020), making it difficult to assess its contribution to Hg(II) methylation.

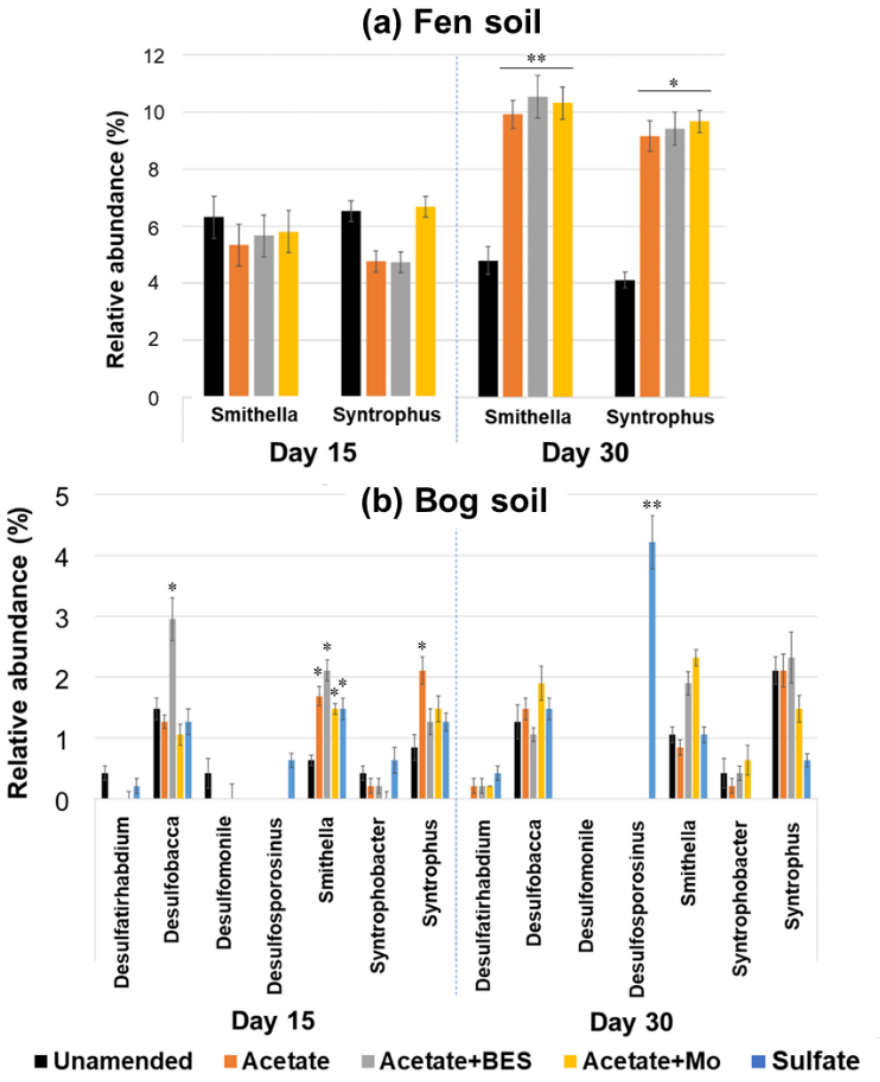

Fig. 3. Changes in relative abundances of microbial guilds containing SRB at the Genus level in the fen (**a**) and bog (**b**) soils either without or with amendments of acetate, acetate+BES, acetate+Mo, or sulfate after 15 and 30 days. Relative abundances were averaged from triplicate incubations with error bars representing one standard deviation. Significant changes with different amendaments at each timepoint are marked as (*) $P<0.05$ and (**) $P<0.01$.

3.4. Microbial community responses to incubation

Philben et al. (2020) previously showed that microbial community compositions before incubation were different between the fen and bog soils used in this study. Beyond the phylum

494 level differences among different bacteria, the composition of methanogenic archaea was
495 significantly different between the fen and bog soils, where the hydrogenotrophic Rice Cluster II
496 dominated the *Euryarchaeota* in the fen soil, while the *Euryarchaeota* in the bog soil were more
497 diverse and contained both acetoclastic and hydrogenotrophic OTUs (Philben et al., 2020). In both
498 soils, microbial guilds containing SRB constituted a small portion of the population (Appendix A
499 Fig. S5) before incubation. *Smithella* and *Syntrophus* containing SRB members (Plugge et al.,
500 2011) were the most abundant genera in both soils, consisting of 12.8±0.2% and 3.8±0.3% of total
501 bacteria in the fen and bog soils, respectively. However, SRB diversity was higher in the bog soil,
502 as OTUs belonging to *Desulfatirhabdium, Desulfobacca, Desulfomonile* and *Syntrophobacter*
503 were also detected in addition to *Smithella* and *Syntrophus* (Appendix A Fig. S5). More diverse
504 methanogenic archaea and SRB in the bog soil than in the fen soil may have contributed to
505 comparable MeHg production in the two soils (Figs. 2a and 2c), overcoming potential limitation
506 of lower concentrations of sulfate and pH in the bog soil (Table 1).

507 Analyses of species richness and β-diversity trends tied to the incubations showed that
508 incubation time and amendments did not significantly change community diversity in both the fen
509 and the bog soils over the course of 30 days (Appendix A Fig. S6). Focusing on microbial
510 populations that are potentially significant to Hg(II) methylation, further analyses showed that
511 microbial community structure response to acetate addition was limited in both soils. Changes in
512 relative abundance of methanogenic archaea were marginal in both soils (Philben et al., 2020). For
513 microbial guilds containing SRB, significant increases in *Smithella* (P=0.003) and *Syntrophus*
514 (P=0.028) abundances were observed in the acetate-amended fen soil at day 30 (Fig. 3a). In the
515 acetate-amended bog soil, similar increases were observed relative to the unamended incubation
516 at day 15, but not at day 30 (Fig. 3b). These different microbial responses suggest that future

studies are needed to further elucidate the mechanisms and interactions of microbial communities, as the two soils differed in pH and sulfate availability (Liu et al., 1999; Schöcke and Schink, 1997). We also note that, in the sulfate-amended bog soils, the relative abundance of *Desulfosporosinus*, a genus of sulfate-reducing *Firmicutes*, significantly increased and became the most dominant SRB following the incubation (Control vs Sulfate: $t_{(17)} = -4.22$, P=0.001) (Fig. 3b), while *Desulfosporosinus* was not detected in the bog soil before incubation (Appendix A Fig. S5). The result is consistent with the observed promoted MeHg production after sulfate amendment in the bog soil (Fig. 2c), as strains of *Desulfosporosinus* have been reported to methylate Hg(II) in acidic habitats (Gilmour et al., 2013). These observations thus corroborate that increased sulfate availability stimulated microbial growth of SRB and the subsequent MeHg production. A recent study also reported that Hg(II) methylating communities at higher sulfate amendments in freshwater lake sediments were dominated by SRB populations (Jones et al., 2020).

Microbial community response to selective inhibitors (BES and molybdate), however, was minor after incubation of the two soils. In the fen soil, while relative abundances of microbial guilds containing SRB increased from day 15 to day 30, especially of *Smithella* (P=0.017) and *Syntrophus* (P=0.038) (Fig. 3a), there were no significant differences observed among the acetate-only, BES-, and molybdate-amended soils (Fig. 3a). Likewise, methanogens remained unchanged among different treatments (Appendix A Fig. S7). In the bog soil, addition of BES and molybdate also did not significantly affect the relative abundances of microbial guilds containing SRB (Fig. 3b) or FeRB *Geobacter* spp. and methanogens (Philben et al., 2020). Compared to the acetate-amended soil, only *Desulfobacca* increased in the BES-amended bog soil after day 15, and *Smithella* increased in both the BES- and Mo-amended bog soil after 30 days. The relatively stable microbial communities with inhibitor amendments may be explained by potential syntrophy that

supports growth and survival of populations, as *Smithella* and *Syntrophus* are known to develop syntrophic interactions with methanogens when sulfate reduction is limited (Plugge et al., 2011). We note that 16S rRNA analysis could not distinguish whether the affected microorganisms are metabolically active or not (Li et al., 2017). However, despite the effects of microbial inhibitors on the overall community structures was insignificant or could not be identified, the inhibitors effectively inhibited sulfate reduction and methanogenesis (Figs. 2b and 2d, and Appendix A Figs. S1 and S4), suggesting important roles of each metabolic group in Hg methylation. Additionally, although acetate concentration was not a limiting factor in MeHg production in these tundra soils, acetate-induced changes in SRB abundances may still affect other biogeochemical processes, such as greenhouse gas production in these soils (Philben et al., 2020).

3.5. Potential microbial drivers of Hg(II) methylation

Arctic tundra is a significant sink of Hg due to its high soil organic matter content and could become an increasingly important source of MeHg to the Arctic ecosystems, as microbial production of MeHg in soil increases upon climate warming (Yang et al., 2016a). Microbial Hg(II) methylation has been associated with diverse groups of predominantly anaerobic bacteria and archaea (Gilmour et al., 2018; Gilmour et al., 2013). While Hg(II) methylation activity has been confirmed experimentally only for a small set of microorganisms, the presence of the genes, *hgcA* and *hgcB*, and their highly conserved sequence motifs correlate well with the ability to methylate Hg(II) (Podar et al., 2015; Schaefer et al., 2020). Therefore, these genes were used as proxies indicating the capacity to methylate Hg(II). Based on the distribution of *hgcA* among sequenced genomes and metagenomes publicly available in IMG/M (as of January 2021), individual Hg(II) methylating species appear to occur across 30 different phyla including several currently designated as candidate phyla (Appendix B). The majority of known methylators are associated

563 with the Deltaproteobacteria, the methanogenic Archaea, and the Firmicutes. Although not all
564 species within a taxon may carry *hgcAB*, the genes are known to be more prevalent within certain
565 clades and environments (Podar et al., 2015). While we identified a total of 12 family level taxa
566 (distributed across 3 phyla) with relative abundances >0.1% that may harbor Hg(II) methylators
567 in the fen and bog reference soils (Fig. 4a), family level abundances indicate that the vast majority
568 of clades that may harbor Hg(II) methylators are within the Proteobacteria (Fig. 4a). On the family
569 level, the Syntrophaceae accounted for 4.8% and 1.4%, respectively, in the reference fen and bog
570 soils before incubation and was among the selected taxa showing the highest relative abundances
571 in both soils (Fig. 4a). The genera *Smithella*, *Syntrophus*, and *Desulfobacca*, which are members
572 of the Synthrophaceae, were observed in both the fen and bog soils (Fig. 3). Other groups in the
573 order of relative abundance were the Syntrophorhabdaceae (0.77%), the Clostridiaceae (0.49%),
574 and the Spirochaetaceae (0.45%) in the fen soil, and the Geobacteraceae (1.3%), the
575 Spirochaetaceae (0.88%), and the Syntrophorhabdaceae (0.42%) in the bog soil.

576 As noted earlier, the addition of acetate led to some changes in the overall microbial
577 community composition (Fig. 3 and Appendix A Fig. S8) between the unamended and acetate-
578 amended fen soils, but minor differences were observed among family-level taxa associated with
579 Hg(II) methylation, except for Hungateiclostridiaceae (Fig. 4a). However, in the bog soil the
580 relative abundance of the Clostridiaceae increased from 2.4% in the unamended soil to 4.8% in
581 the acetate-amended soil after 60 days (Fig. 4a). Although Hg(II) methylators are shown in seven
582 genera among the Clostridiaceae (Appendix B), none of these specific genera appear to be present
583 in the fen or bog soils (Appendix A Fig. S9), which suggests that the observed increase in the
584 abundance of the Clostridiaceae should not impact MeHg production. The Geobacteraceae
585 decreased from 2.9% in the unamended bog soil to 0.9% in the acetate-amended soil after 60 days

(Fig. 4a), although MeHg production was not impacted either with or without the addition of acetate (Fig. 2c). The presence of FeRB *Geobacter* was also detected (Appendix A Fig. S9), but a small decrease in their relative abundances was observed during incubation, suggesting that FeRB unlikely played an important role in Hg(II) methylation either. This result appears contradicting to a previous study, in which *Geobacteraceae* were thought to be important Hg(II) methylators in wetland soils (Schaefer et al., 2020). We therefore suggest that future studies are performed to further determining the role of FeRB in MeHg production, particularly when sulfate availability is limited in these soils. However, amendment with sulfate in the bog soil substantially increased the relative abundance of sulfate-reducing Clostridia, specifically the family Peptococcaceae (Fig. 4b), which harbors the genus *Desulfosporosinus* (Appendix A Fig. S10) containing 11 species carrying the *hgcA* gene essential for Hg(II) methylation (Appendix B). The relative abundances of other groups capable of sulfate reduction (e.g. the Syntrophaceae) did not change or decreased slightly (Fig. 4b). The results again suggest that metabolic interdependencies of syntrophic microorganisms might play an important role in driving the production of MeHg in these soils. We caution, however, that these estimates based on 16S rRNA gene results may have limitations with respect to DNA extraction method, primers, PCR cycles, and even the differences in 16S rRNA gene copy numbers per genome may impact identification of microbial communities and their abundances (Pollock et al., 2018). Future studies using more advanced and direct techniques (e.g., transcriptomics) targeting syntrophic species carrying *hgcAB* are thus warranted to reveal additional factors controlling MeHg production in these arctic soils (Barkay and Poulain, 2007; Grégoire and Poulain, 2018; Yu et al., 2018).

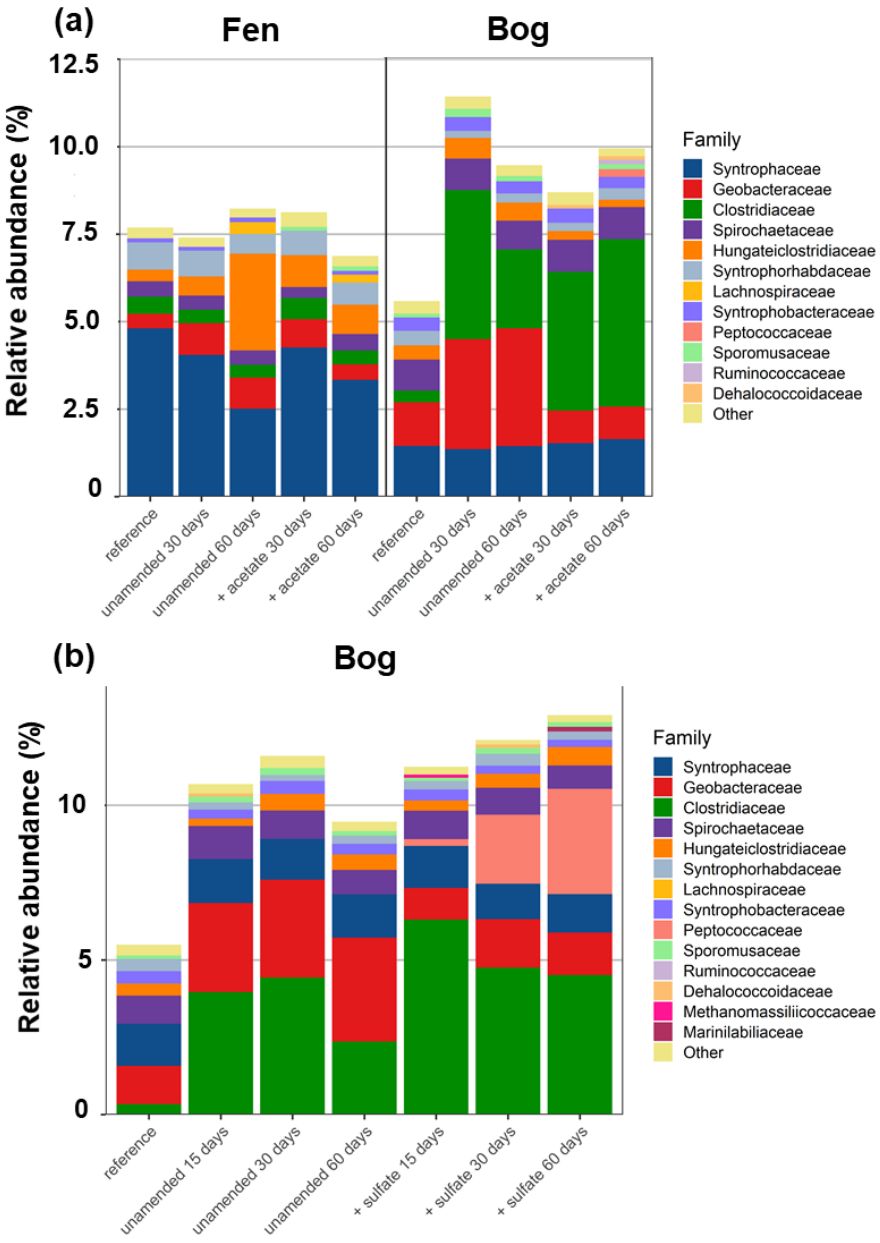

607

608 **Fig. 4**. Relative abundances of taxa associated with Hg(II) methylation at the family level in the
609 fen and bog soils. Families at levels of less than 0.1% were combined into the group "Other". (**a**)
610 Reference soils before incubation, unamended and acetate-amended soils after 30 and 60 days of
611 incubation. The relative abundance of individual taxa ranged from < 0.001 % to 4.8% in the fen
612 soil and from < 0.006 % to 4.8 % in the bog soil. (**b**) Effect of sulfate amendment on relative
613 abundances (> 0.1%) of taxa associated with Hg(II) methylation at the family level in bog soil
614 incubations.

3. Conclusions

Overall, our microcosm incubation experiments demonstrated that MeHg production in the tundra soil was not limited by acetate but sulfate availability, particularly in the bog soil with a low sulfate concentration. Increasing acetate concentration did not affect MeHg production, but sulfate addition significantly promoted MeHg production likely through stimulation of Hg(II) methylating SRB. Sulfate amendment in the bog soil incubations increased the relative abundance of Firmicutes, specifically the genus *Desulfosporosinus*. Our results indicate that the dominant microbial groups for Hg(II) methylation were dependent on soil geochemistry. In the fen soil, SRB appeared to be the predominant microbes in producing MeHg when sufficient amounts of sulfate were available. In contrast, both methanogens and SRB contributed to MeHg production directly and/or indirectly, possibly through syntrophic interactions when sulfate was limited. Together, these results reveal potential biogeochemical drivers of MeHg production in the Arctic tundra soils, an important step to advance our understanding of the transformation and bioaccumulation of Hg and MeHg in the rapidly changing Arctic ecosystem due to climate warming.

Appendix A. Supplementary Information

Changes in methane, acetate, sulfate, and methylmercury concentrations in the fen and bog soil incubations; $Me^{202}Hg$ concentrations over the course of demethylation experiments; Relative abundance of SRBs at *Genus* level in the fen and bog soils before incubation; Changes in species richness and diversity in the fen and bog soils after incubations for 30 day; Relative abundance of identified taxa at the phylum level in soil incubations after 60 days; Relative abundance of taxa (> 0.1%) associated with Hg(II) methylation at the genus level in unamended and acetate-amended fen and bog soil incubations after 60 days; Relative abundance of taxa (> 0.1%) associated with

Hg(II) methylation at the family level in unamended and sulfate-amended bogl soil incubations; Incubation experimental setups and concentrations of amendments.

Appendix B. Supplementary Data

Genome IDs and description of microbial species with confirmed *hgcA* marker genes obtained from the Joint Genome Institute's IMG/M database and derived taxonomic lineages with Hg methylating microorganisms. Both Appendix A and B to this article can be found online at https://doi XXXX.

Notes: The authors declare no competing financial interest.

Acknowledgments

We thank Xiangping Yin for technical support in Hg and MeHg analyses. This research was sponsored by the Office of Biological and Environmental Research within the Office of Science of the U.S. Department of Energy (DOE), as part of the Mercury Science Focus Area project at the Oak Ridge National Laboratory (ORNL). The Hg isotopes used in this research were supplied by DOE Office of Science the Isotope Program in the Office of Nuclear Physics. DOE will provide public access to these results of federally sponsored research in accordance with the DOE Public Access Plan (http://energy.gov/downloads/doe-public-access-plan). ORNL is managed by UT-Battelle, LLC under Contract No. DE-AC05-00OR22725 with DOE.

References

Åkerblom, S., Nilsson, M.B., Skyllberg, U., Björn, E., Jonsson, S., Ranneby, B., Bishop, K., 2020. Formation and mobilization of methylmercury across natural and experimental sulfur deposition gradients. Environmental Pollution: 114398.

Alli, A., Jaffé, R., Jones, R., 1994. Analysis of organomercury compounds in sediments by capillary GC with atomic fluorescence detection. Journal of High Resolution Chromatography, 17(11): 745-748.

Antelo, J., Fiol, S., Gondar, D., López, R., Arce, F., 2012. Comparison of arsenate, chromate and molybdate binding on schwertmannite: Surface adsorption vs anion-exchange. Journal of colloid and interface science, 386(1): 338-343.

Barkay, T., Gu, B., 2021. Demethylation─The Other Side of the Mercury Methylation Coin: A Critical Review. ACS Environmental Au.

Barkay, T., Poulain, A.J., 2007. Mercury (micro)biogeochemistry in polar environments. FEMS Microbiology Ecology, 59(2): 232-241.

Bates, D., Mächler, M., Bolker, B., Walker, S., 2014. Fitting linear mixed-effects models using lme4. arXiv preprint arXiv:1406.5823.

Biswas, K.C., Woodards, N.A., Xu, H., Barton, L.L., 2009. Reduction of molybdate by sulfate-reducing bacteria. Biometals, 22(1): 131-139.

Bloom, N.S., Colman, J.A., Barber, L., 1997. Artifact formation of methyl mercury during aqueous distillation and alternative techniques for the extraction of methyl mercury from environmental samples. Fresenius' Journal of Analytical Chemistry, 358(3): 371-377.

Bloom, N.S., Preus, E., Katon, J., Hiltner, M., 2003. Selective extractions to assess the biogeochemically relevant fractionation of inorganic mercury in sediments and soils. Analytica Chimica Acta, 479(2): 233-248.

Bokulich, N.A., Subramanian, S., Faith, J.J., Gevers, D., Gordon, J.I., Knight, R., Mills, D.A., Caporaso, J.G., 2013. Quality-filtering vastly improves diversity estimates from Illumina amplicon sequencing. Nature methods, 10(1): 57-59.

Bravo, A.G., Peura, S., Buck, M., Ahmed, O., Mateos-Rivera, A., Ortega, S.H., Schaefer, J.K., Bouchet, S., Tolu, J., Björn, E., 2018. Methanogens and iron-reducing bacteria: the overlooked members of mercury-methylating microbial communities in boreal lakes. Appl. Environ. Microbiol., 84(23): e01774-18.

Bray, J.R., Curtis, J.T., 1957. An ordination of the upland forest communities of southern Wisconsin. Ecological monographs, 27(4): 325-349.

Bridou, R., Monperrus, M., Gonzalez, P.R., Guyoneaud, R., Amouroux, D., 2011. Simultaneous determination of mercury methylation and demethylation capacities of various sulfate-reducing bacteria using species-specific isotopic tracers. Environmental toxicology and chemistry, 30(2): 337-344.

Caporaso, J.G., Kuczynski, J., Stombaugh, J., Bittinger, K., Bushman, F.D., Costello, E.K., Fierer, N., Pena, A.G., Goodrich, J.K., Gordon, J.I., 2010. QIIME allows analysis of high-throughput community sequencing data. Nature methods, 7(5): 335-336.

Caporaso, J.G., Lauber, C.L., Walters, W.A., Berg-Lyons, D., Lozupone, C.A., Turnbaugh, P.J., Fierer, N., Knight, R., 2011. Global patterns of 16S rRNA diversity at a depth of millions of sequences per sample. Proceedings of the National Academy of Sciences, 108(Supplement 1): 4516-4522.

Chamberlain, S.A., Szöcs, E., 2013. taxize: taxonomic search and retrieval in R. F1000Research, 2.

Cooper, C.J., Zheng, K., Rush, K.W., Johs, A., Sanders, B.C., Pavlopoulos, G.A., Kyrpides, N.C., Podar, M., Ovchinnikov, S., Ragsdale, S.W., 2020. Structure determination of the HgcAB complex using metagenome sequence data: insights into microbial mercury methylation. Communications biology, 3(1): 1-9.

Dang, C., Morrissey, E.M., Neubauer, S.C., Franklin, R.B., 2019. Novel microbial community composition and carbon biogeochemistry emerge over time following saltwater intrusion in wetlands. Global Change Biology, 25(2): 549-561.

Drake, T.W., Wickland, K.P., Spencer, R.G.M., McKnight, D.M., Striegl, R.G., 2015. Ancient low–molecular-weight organic acids in permafrost fuel rapid carbon dioxide production upon thaw. Proceedings of the National Academy of Sciences, 112(45): 13946-13951.

Edgar, R.C., 2013. UPARSE: highly accurate OTU sequences from microbial amplicon reads. Nature methods, 10(10): 996-998.

Furutani, A., Rudd, J.W., 1980. Measurement of mercury methylation in lake water and sediment samples. Applied and environmental microbiology, 40(4): 770-776.

Gilmour, C.C., Bullock, A.L., McBurney, A., Podar, M., Elias, D.A., 2018. Robust mercury methylation across diverse methanogenic Archaea. MBio, 9(2).

Gilmour, C.C., Henry, E.A., Mitchell, R., 1992. Sulfate stimulation of mercury methylation in freshwater sediments. Environmental Science & Technology, 26(11): 2281-2287.

Gilmour, C.C., Podar, M., Bullock, A.L., Graham, A.M., Brown, S.D., Somenahally, A.C., Johs, A., Hurt Jr, R.A., Bailey, K.L., Elias, D.A., 2013. Mercury methylation by novel microorganisms from new environments. Environmental Science & Technology, 47(20): 11810-11820.

Grégoire, D.S., Poulain, A.J., 2018. Shining light on recent advances in microbial mercury cycling. Facets, 3(1): 858-879.

Hamelin, S., Amyot, M., Barkay, T., Wang, Y., Planas, D., 2011. Methanogens: Principal Methylators of Mercury in Lake Periphyton. Environmental Science & Technology, 45(18): 7693-7700.

Hamelin, S., Planas, D., Amyot, M., 2015. Mercury methylation and demethylation by periphyton biofilms and their host in a fluvial wetland of the St. Lawrence River (QC, Canada). Science of the Total Environment, 512: 464-471.

Hausmann, B., Knorr, K.-H., Schreck, K., Tringe, S.G., Glavina del Rio, T., Loy, A., Pester, M., 2016. Consortia of low-abundance bacteria drive sulfate reduction-dependent degradation of fermentation products in peat soil microcosms. The ISME Journal, 10(10): 2365-2375.

Hintelmann, H., Ogrinc, N., 2002. Determination of Stable Mercury Isotopes by ICP/MS and Their Application in Environmental Studies, Biogeochemistry of Environmentally Important Trace Elements. ACS Symposium Series. American Chemical Society, pp. 321-338.

Hu, H., Wang, B., Bravo, A.G., Björn, E., Skyllberg, U., Amouroux, D., Tessier, E., Zopfi, J., Feng, X., Bishop, K., Nilsson, M.B., Bertilsson, S., 2020. Shifts in mercury methylation across a peatland chronosequence: From sulfate reduction to methanogenesis and syntrophy. Journal of Hazardous Materials, 387: 121967.

Jones, D.S., Johnson, N.W., Mitchell, C.P.J., Walker, G.M., Bailey, J.V., Pastor, J., Swain, E.B., 2020. Diverse Communities of hgcAB+ Microorganisms Methylate Mercury in Freshwater Sediments Subjected to Experimental Sulfate Loading. Environmental Science & Technology, 54(22): 14265-14274.

Kim, Y., Lee, B.-Y., Suzuki, R., Kushida, K., 2016. Spatial characteristics of ecosystem respiration in three tundra ecosystems of Alaska. Polar Science, 10(3): 356-363.

Kirk, J.L., Lehnherr, I., Andersson, M., Braune, B.M., Chan, L., Dastoor, A.P., Durnford, D., Gleason, A.L., Loseto, L.L., Steffen, A., 2012. Mercury in Arctic marine ecosystems: Sources, pathways and exposure. Environmental research, 119: 64-87.

Kronberg, R.-M., Schaefer, J.K., Björn, E., Skyllberg, U., 2018. Mechanisms of Methyl Mercury Net Degradation in Alder Swamps: The Role of Methanogens and Abiotic Processes. Environmental Science & Technology Letters, 5(4): 220-225.

751 Léger, E., Dafflon, B., Robert, Y., Ulrich, C., Peterson, J.E., Biraud, S.C., Romanovsky, V.E., Hubbard,
752 S.S., 2019. A distributed temperature profiling method for assessing spatial variability in ground
753 temperatures in a discontinuous permafrost region of Alaska. The Cryosphere, 13(11): 2853-
754 2867.

755 Lehnherr, I., 2014. Methylmercury biogeochemistry: a review with special reference to Arctic aquatic
756 ecosystems. Environmental Reviews, 22(3): 229-243.

757 Lehnherr, I., St. Louis, V.L., Kirk, J.L., 2012. Methylmercury Cycling in High Arctic Wetland Ponds:
758 Controls on Sedimentary Production. Environmental Science & Technology, 46(19): 10523-
759 10531.

760 Li, R., Tun, H.M., Jahan, M., Zhang, Z., Kumar, A., Fernando, W.D., Farenhorst, A., Khafipour, E., 2017.
761 Comparison of DNA-, PMA-, and RNA-based 16S rRNA Illumina sequencing for detection of
762 live bacteria in water. Scientific reports, 7(1): 1-11.

763 Lin, H., Morrell-Falvey, J.L., Rao, B., Liang, L., Gu, B., 2014. Coupled mercury–cell sorption, reduction,
764 and oxidation on methylmercury production by Geobacter sulfurreducens PCA. Environmental
765 Science & Technology, 48(20): 11969-11976.

766 Liu, Y.-R., Johs, A., Bi, L., Lu, X., Hu, H.-W., Sun, D., He, J.-Z., Gu, B., 2018. Unraveling Microbial
767 Communities Associated with Methylmercury Production in Paddy Soils. Environmental Science
768 & Technology, 52(22): 13110-13118.

769 Liu, Y., Balkwill, D.L., Aldrich, H.C., Drake, G.R., Boone, D.R., 1999. Characterization of the anaerobic
770 propionate-degrading syntrophs Smithella propionica gen. nov., sp. nov. and Syntrophobacter
771 wolinii. International Journal of Systematic and Evolutionary Microbiology, 49(2): 545-556.

772 Loseto, L.L., Siciliano, S.D., Lean, D.R.S., 2004. Methylmercury production in high arctic wetlands.
773 Environmental Toxicology and Chemistry, 23(1): 17-23.

774 Lu, X., Gu, W., Zhao, L., Haque, M.F.U., DiSpirito, A.A., Semrau, J.D., Gu, B., 2017. Methylmercury
775 uptake and degradation by methanotrophs. Science advances, 3(5): e1700041.

776 Lu, X., Zhao, J., Liang, X., Zhang, L., Liu, Y., Yin, X., Li, X., Gu, B., 2019. The application and potential
777 artifacts of Zeeman cold Vapor atomic absorption spectrometry in mercury stable isotope
778 analysis. Environmental Science & Technology Letters, 6(3): 165-170.

779 Luo, H.-W., Yin, X., Jubb, A.M., Chen, H., Lu, X., Zhang, W., Lin, H., Yu, H.-Q., Liang, L., Sheng, G.-
780 P., Gu, B., 2017. Photochemical reactions between mercury (Hg) and dissolved organic matter
781 decrease Hg bioavailability and methylation. Environmental Pollution, 220: 1359-1365.

782 MacMillan, G.A., Girard, C., Chételat, J., Laurion, I., Amyot, M., 2015. High Methylmercury in Arctic
783 and Subarctic Ponds is Related to Nutrient Levels in the Warming Eastern Canadian Arctic.
784 Environmental Science & Technology, 49(13): 7743-7753.

785 Magoč, T., Salzberg, S.L., 2011. FLASH: fast length adjustment of short reads to improve genome
786 assemblies. Bioinformatics, 27(21): 2957-2963.

787 McMurdie, P.J., Holmes, S., 2013. phyloseq: an R package for reproducible interactive analysis and
788 graphics of microbiome census data. PloS one, 8(4): e61217.

789 Miller, C.L., Southworth, G., Brooks, S., Liang, L., Gu, B., 2009. Kinetic controls on the complexation
790 between mercury and dissolved organic matter in a contaminated environment. Environmental
791 Science & Technology, 43(22): 8548-8553.

792 Miller, C.L., Watson, D.B., Lester, B.P., Lowe, K.A., Pierce, E.M., Liang, L., 2013. Characterization of
793 soils from an industrial complex contaminated with elemental mercury. Environmental research,
794 125: 20-29.

Mitchell, C.P.J., Branfireun, B.A., Kolka, R.K., 2008. Assessing sulfate and carbon controls on net methylmercury production in peatlands: An in situ mesocosm approach. Applied Geochemistry, 23(3): 503-518.

Obrist, D., Agnan, Y., Jiskra, M., Olson, C.L., Colegrove, D.P., Hueber, J., Moore, C.W., Sonke, J.E., Helmig, D., 2017. Tundra uptake of atmospheric elemental mercury drives Arctic mercury pollution. Nature, 547(7662): 201.

Oksanen, J., Blanchet, F.G., Kindt, R., Legendre, P., Minchin, P., O'hara, R., Simpson, G., Solymos, P., Stevens, M., Wagner, H., 2013. Community ecology package. R package version, 2(0).

Olsen, T.A., Brandt, C.C., Brooks, S.C., 2016. Periphyton biofilms influence net methylmercury production in an industrially contaminated system. Environmental Science & Technology, 50(20): 10843-10850.

Parks, J.M., Johs, A., Podar, M., Bridou, R., Hurt, R.A., Smith, S.D., Tomanicek, S.J., Qian, Y., Brown, S.D., Brandt, C.C., Palumbo, A.V., Smith, J.C., Wall, J.D., Elias, D.A., Liang, L., 2013. The genetic basis for bacterial mercury methylation. Science, 339(6125): 1332-1335.

Patil, I., ; Powell, C.; Beasley, W.; Heck, D.; Hvitfeldt, E., **2019**. ggstatsplot: Compatibility with 'ggplot2 3.3.0', Zenodo.

Philben, M., Zhang, L., Yang, Z., Taş, N., Wullschleger, S.D., Graham, D.E., Gu, B., 2020. Anaerobic respiration pathways and response to increased substrate availability of Arctic wetland soils. Environ. Sci. Process Impacts, 22(10): 2070-2083.

Philben, M., Zheng, J., Bill, M., Heikoop, J.M., Perkins, G., Yang, Z., Wullschleger, S.D., Graham, D.E., Gu, B., 2019. Stimulation of anaerobic organic matter decomposition by subsurface organic N addition in tundra soils. Soil Biology and Biochemistry, 130: 195-204.

Plugge, C.M., Zhang, W., Scholten, J., Stams, A.J., 2011. Metabolic flexibility of sulfate-reducing bacteria. Frontiers in microbiology, 2: 81.

Podar, M., Gilmour, C.C., Brandt, C.C., Soren, A., Brown, S.D., Crable, B.R., Palumbo, A.V., Somenahally, A.C., Elias, D.A., 2015. Global prevalence and distribution of genes and microorganisms involved in mercury methylation. Science advances, 1(9): e1500675.

Pollock, J., Glendinning, L., Wisedchanwet, T., Watson, M., 2018. The madness of microbiome: attempting to find consensus "best practice" for 16S microbiome studies. Applied and environmental microbiology, 84(7): e02627-17.

Price, M.N., Dehal, P.S., Arkin, A.P., 2010. FastTree 2–approximately maximum-likelihood trees for large alignments. PloS one, 5(3): e9490.

Quast, C., Pruesse, E., Yilmaz, P., Gerken, J., Schweer, T., Yarza, P., Peplies, J., Glöckner, F.O., 2012. The SILVA ribosomal RNA gene database project: improved data processing and web-based tools. Nucleic acids research, 41(D1): D590-D596.

Schaefer, J.K., Kronberg, R.-M., Björn, E., Skyllberg, U., 2020. Anaerobic guilds responsible for mercury methylation in boreal wetlands of varied trophic status serving as either a methylmercury source or sink. Environmental Microbiology, 22(9).

Schartup, A.T., Balcom, P.H., Soerensen, A.L., Gosnell, K.J., Calder, R.S., Mason, R.P., Sunderland, E.M., 2015. Freshwater discharges drive high levels of methylmercury in Arctic marine biota. Proceedings of the National Academy of Sciences, 112(38): 11789-11794.

Schöcke, L., Schink, B., 1997. Energetics of methanogenic benzoate degradation by Syntrophus gentianae in syntrophic coculture. Microbiology, 143(7): 2345-2351.

838 Schuster, P.F., Schaefer, K.M., Aiken, G.R., Antweiler, R.C., Dewild, J.F., Gryziec, J.D., Gusmeroli, A.,
839 Hugelius, G., Jafarov, E., Krabbenhoft, D.P., 2018. Permafrost stores a globally significant
840 amount of mercury. Geophysical Research Letters, 45(3): 1463-1471.

841 Schwartz, G.E., Olsen, T.A., Muller, K.A., Brooks, S.C., 2019. Ecosystem controls on methylmercury
842 production by periphyton biofilms in a contaminated stream: implications for predictive
843 modeling. Environmental toxicology and chemistry, 38(11): 2426-2435.

844 St. Pierre, K., Chételat, J., Yumvihoze, E., Poulain, A., 2014. Temperature and the sulfur cycle control
845 monomethylmercury cycling in high Arctic coastal marine sediments from Allen Bay, Nunavut,
846 Canada. Environmental science & technology, 48(5): 2680-2687.

847 Team, R.C., 2013. R: A language and environment for statistical computing. R Foundation for Statistical
848 Computing, Vienna.

849 Tully, K.L., Weissman, D., Wyner, W.J., Miller, J., Jordan, T., 2019. Soils in transition: saltwater
850 intrusion alters soil chemistry in agricultural fields. Biogeochemistry, 142(3): 339-356.

851 Wang, Q., Garrity, G.M., Tiedje, J.M., Cole, J.R., 2007. Naive Bayesian classifier for rapid assignment of
852 rRNA sequences into the new bacterial taxonomy. Applied and environmental microbiology,
853 73(16): 5261-5267.

854 Wang, Q., Zhang, L., Liang, X., Yin, X., Zhang, Y., Zheng, W., Pierce, E.M., Gu, B., 2020. Rates and
855 Dynamics of Mercury Isotope Exchange between Dissolved Elemental Hg(0) and Hg(II) Bound
856 to Organic and Inorganic Ligands. Environmental Science & Technology, 54(23): 15534-15545.

857 Woodcroft, B.J., Singleton, C.M., Boyd, J.A., Evans, P.N., Emerson, J.B., Zayed, A.A.F., Hoelzle, R.D.,
858 Lamberton, T.O., McCalley, C.K., Hodgkins, S.B., Wilson, R.M., Purvine, S.O., Nicora, C.D., Li,
859 C., Frolking, S., Chanton, J.P., Crill, P.M., Saleska, S.R., Rich, V.I., Tyson, G.W., 2018.
860 Genome-centric view of carbon processing in thawing permafrost. Nature, 560(7716): 49-54.

861 Yang, Z., Fang, W., Lu, X., Sheng, G.-P., Graham, D.E., Liang, L., Wullschleger, S.D., Gu, B., 2016a.
862 Warming increases methylmercury production in an Arctic soil. Environmental Pollution, 214:
863 504-509.

864 Yang, Z., Wullschleger, S.D., Liang, L., Graham, D.E., Gu, B., 2016b. Effects of warming on the
865 degradation and production of low-molecular-weight labile organic carbon in an Arctic tundra
866 soil. Soil Biology and Biochemistry, 95: 202-211.

867 Yang, Z., Yang, S., Van Nostrand, J.D., Zhou, J., Fang, W., Qi, Q., Liu, Y., Wullschleger, S.D., Liang, L.,
868 Graham, D.E., Yang, Y., Gu, B., 2017. Microbial Community and Functional Gene Changes in
869 Arctic Tundra Soils in a Microcosm Warming Experiment. Frontiers in Microbiology, 8(1741).

870 Yu, R.-Q., Reinfelder, J.R., Hines, M.E., Barkay, T., 2013. Mercury methylation by the methanogen
871 Methanospirillum hungatei. Appl. Environ. Microbiol., 79(20): 6325-6330.

872 Yu, R.-Q., Reinfelder, J.R., Hines, M.E., Barkay, T., 2018. Syntrophic pathways for microbial mercury
873 methylation. The ISME journal, 12(7): 1826-1835.

874 Zaporski, J., Jamison, M., Zhang, L., Gu, B., Yang, Z., 2020. Mercury methylation potential in a sand
875 dune on Lake Michigan's eastern shoreline. Science of The Total Environment, 729: 138879.

876 Zhang, L., Liang, X., Wang, Q., Zhang, Y., Yin, X., Lu, X., Pierce, E.M., Gu, B., 2021. Isotope exchange
877 between mercuric [Hg(II)] chloride and Hg(II) bound to minerals and thiolate ligands:
878 Implications for enriched isotope tracer studies. Geochim. Cosmochim. Acta, 292: 468-481.

879 Zhang, L., Wu, S., Zhao, L., Lu, X., Pierce, E.M., Gu, B., 2019. Mercury sorption and desorption on
880 organo-mineral particulates as a source for microbial methylation. Environmental Science &
881 Technology, 53(5): 2426-2433.